Ergodic property of a Henon-Heiles model with reflecting walls

Zhigang Zheng,[1] Gang Hu,[1,2] and Juyuan Zhang[1,3]
[1]*Physics Department, Beijing Normal University, Beijing 100875, China*
[2]*Center of Theoretical Physics, Chinese Center of Advanced Science and Technology (World Laboratory), Beijing 8730, China*
[3]*Physics Department, Siping Teacher's College, Jilin 136000, China*
(Received 5 April 1995)

A modified Henon-Heiles model with reflecting walls is suggested to discuss the ergodic property of the motion of a two-dimensional oscillator with nonlinear coupling. A quantitative method for estimating the ergodicity of a chaotic trajectory is proposed in terms of a microcanonical distribution. The influence of the boundary on the ergodic and chaotic behavior is discussed. Our investigations show that, by adjusting the distance and the shape of the boundary, a simple Henon-Heiles system can reach ergodicity on the constant-energy surface, and therefore various concepts in traditional statistical physics can be introduced into this simple system.

PACS number(s): 05.45.+b, 02.50.−r

I. HENON-HEILES MODEL WITH REFLECTING WALLS

Ergodicity, i.e., the exploration of the energy surface $H(p,q)=E$ by a typical trajectory, is at the very foundation of statistical mechanics [1–4]. It has been shown that for ergodic Hamiltonian systems ergodicity (chaos) provides the validity of the laws of equilibrium thermodynamics and statistical mechanics [5]. In traditional hypotheses, this property is always connected to a large number of degrees of freedom and cannot be proved. The subject of ergodic theory was primarily the domain of mathematicians until the advent of modern computers. In the late 20th century, with the wide exploration of nonintegrable systems and chaos, studies of ergodicity in small systems with only a few degrees of freedom have become an exciting subject. The importance of this subject lies in that it builds a bridge between traditional mechanics and statistical physics.

As to ergodicity (or stronger properties such as mixing, K flow, and so on), the most extensively investigated system is the Sinai billiard [6,7]. A particle moves freely in a container and is reflected elastically on the walls. As long as the boundary is weakly asymmetric (e.g., by cutting off an arc on the circular boundary or cutting off a small fan at one of the corners of the triangular boundary), chaotic motion and ergodicity on the constant-energy surface can be achieved. For this system, ergodicity (and mixing, K flow) has been theoretically and numerically studied [6–11].

The Sinai billiard is a very special physical system. Many Hamiltonian systems with nonlinear potentials correspond to billiard systems in the high-energy limit, but the study of ergodicity for intermediate- and low-energy cases is still inadequate [12]. Therefore it is necessary to extend the discussion of ergodicity to general systems such as anharmonic oscillator systems. To date the only models amenable to algebraic studies are those with integrable or near integrable Hamiltonians. Integrability conditions rule out ergodicity. The failure of the algebraic approach emphasizes the importance of numerical investigation [13]. The most widely discussed coupled oscillator system is the Henon-Heiles model [14–16], which has the Hamiltonian

$$H=\tfrac{1}{2}(p_1^2+p_2^2+q_1^2+q_2^2)+q_1^2q_2-\tfrac{1}{3}q_2^3 \ . \tag{1}$$

The corresponding canonical equation reads

$$\dot{p}_1=-q_1-2q_1q_2, \quad \dot{p}_2=-q_2+q_2^2-q_1^2 \ , \qquad \dot{q}_1=p_1, \quad \dot{q}_2=p_2 \ . \tag{2}$$

This is a rather old model well known to many physicists, mathematicians, and chemists, because it describes many problems in physics and chemistry [3]. Numerical explorations revealed that for $E<\frac{1}{12}$ the motion of the system is regular. With increasing energy, Kolmogorov-Arnol'd-Moser (KAM) tori are destroyed gradually, and the chaotic region becomes larger. At $E=\frac{1}{6}$, the motion is almost completely chaotic. Therefore the Henon-Heiles model is an excellent candidate for the discussion of the relationship between dynamics and statistical mechanics. People expect that ergodicity on the energy surface will be achieved with increasing energy E. However, two drawbacks exist in this model: first, the maximum energy of this system is $E=\frac{1}{6}$. When $E>\frac{1}{6}$, the oscillator tends to escape from the saddle points $[(q_1,q_2)=(0,1), \ (\pm\sqrt{3}/2,-\frac{1}{2})]$, and hence numerical computation will overflow. Second, the system is not ergodic on the energy surface even at $E=\frac{1}{6}$; some KAM tori still remain at this highest energy. Moreover, few good quantitative standards have been used to estimate the ergodicity of a system. The traditional method for estimating the degree of ergodicity is to compute the percentage of the number of chaotic trajectories in N randomly selected initial conditions [3,14]. This method needs a long running time and is not accurate.

In order to discuss the statistical behavior (ergodicity) of the Henon-Heiles system for various energies, we suggest a modified Henon-Heiles model with reflecting walls

ϵ; thus the motion of the particle will be restricted inside a given domain and completely elastic collisions occur on the boundary. The Hamiltonian then becomes

$$H=\begin{cases}\frac{1}{2}(p_1^2+p_2^2+q_1^2+q_2^2)+q_1^2q_2-\frac{1}{3}q_2^3 & \text{(inside } \epsilon\text{)}\\ \infty & \text{(outside } \epsilon\text{)} .\end{cases} \tag{3}$$

Very rich interesting dynamic behaviors exist in this system, which are affected by both the nonlinear coupling between the oscillators and the shape of the walls. Above all, the dimension of the boundary may affect the motion of the system. For fixed energy, the larger the boundary is, the more the motion of the system approaches that of an unbounded Henon-Heiles system. On the other hand, the shape of the boundary strongly affects the motion of the system, e.g., by changing the form of the wall, a regular (chaotic) motion may change into a chaotic (regular) one. At low energy, the system corresponds to the standard Henon-Heiles model; in the high-energy limit, the boundary-restricted Henon-Heiles model becomes a billiard. In these two limits, the dynamic and statistical behaviors have already been fully discussed, whereas the intermediate behavior is still not systematically investigated.

By constructing a modified model, we can investigate the ergodic behavior of the Henon-Heiles system for various energy cases. Moreover, after introducing the reflecting boundaries, we may obtain additional interesting results. In the next section, we suggest a quantitative method for judging the degree of ergodicity by comparing the cross section distribution generated by a single chaotic trajectory and the equilibrium microcanonical distribution. This measured quantity has good physical meaning and can be obtained by measuring only a single chaotic trajectory.

II. MICROCANONICAL DISTRIBUTION AND ITS MEASUREMENT IN CROSS SECTION

In order to estimate the degree for a chaotic trajectory to cover the energy surface, we propose a method of comparing the cross section distribution and the microcanonical ensemble. Taking the Hamiltonian system with two degrees of freedom for an example, if the system is ergodic, the microcanonical distribution should be

$$\Delta W \propto \Delta p_1 \Delta p_2 \Delta q_1 \Delta q_2 = \Delta\Gamma , \tag{4}$$

where ΔW is the probability of a trajectory entering a phase volume unit $\Delta\Gamma$ between the $E \to E+\Delta E$ energy shells. On the energy surface, $\Delta E \to 0$. By eliminating p_1, the probability distribution becomes

$$\Delta\rho \propto \frac{1}{|\partial H/\partial p_1|}\Delta p_2 \Delta q_1 \Delta q_2 = \frac{1}{|\partial H/\partial p_1|}\Delta V . \tag{5}$$

This is the probability of a trajectory visiting the phase volume ΔV. In order to derive the cross section (for a chaotic trajectory to cross a surface, e.g., $q_1=0$) distribution $D(q_2,p_2)$, we use the definition of ergodicity, i.e., the equality of the temporal average and the phase average:

$$\lim_{T\to\infty}\frac{1}{T}\int_0^T A(p,q)dt = \int A(p,q)\frac{C}{|\partial H/\partial p_1|}dp_2 dq_1 dq_2 . \tag{6}$$

The left side represents the average along a trajectory, and the right one is the average of the microcanonical ensemble. $A(p,q)$ is an arbitrary physical quantity, and C is the normalization constant. Near $q_1=0$, the left side becomes

$$\begin{aligned} A(p,q)dt &= A(p,q)D(q_2,p_2)dq_2dp_2dt \\ &= A(p,q)\frac{D(q_2,p_2)}{|\dot{q}_1|}dq_1dq_2dp_2 \\ &= A(p,q)\frac{D(q_2,p_2)}{|\partial H/\partial p_1|}dp_2dq_1dq_2 . \end{aligned} \tag{7}$$

A comparison of (6) and (7) leads to

$$D(q_2,p_2)=C . \tag{8}$$

This result is independent of the detailed form of the Hamiltonian $H(p,q)$. Note that $D(q_2,p_2)$ is a two-dimensional distribution function, i.e., a cross section density on the $q_1=0$ hypersurface. A general form of $D(s)$ is

$$D(s)=C\frac{|\partial H/\partial A_i|}{|\partial H/\partial B_j|} , \tag{9}$$

which represents the cross section distribution of the two variables other than $\overline{A}_i$ and B_j on the $\overline{A}_i$ hypersurface after the elimination of B_j, where $i,j=1,2$, A or B may be q or p, and $\overline{A},\overline{B}$ are conjugate variables of A,B.

First we investigate the distribution on the section $q_1=0$, $D(q_2,p_2)$. In order to simplify the numerical computation, we define $d(q_2)dq_2$ as the number of the crossing points by which a trajectory enters the interval $q_2 \to q_2+dq_2$ on the q_1 section, thus

$$\begin{aligned} d(q_2) &= \int_{p_{\min}}^{p_{\max}} D(q_2,p_2)dp_2 \\ &= C\{p_{\max}(q_2)-p_{\min}(q_2)\} , \end{aligned} \tag{10}$$

where $p_{\max}$ and $p_{\min}$ are the maximum and minimum of p_2 on the constant-energy surface $H=E$ and $q_1=0$. The above results are valid for arbitrary Hamiltonians with two degrees of freedom. For the Henon-Heiles case, we have

$$\begin{aligned} &p_{\max}=\sqrt{2E-q_2^2+\tfrac{2}{3}q_2^3}, \quad p_{\min}=-\sqrt{2E-q_2^2+\tfrac{2}{3}q_2^3} , \\ &d(q_2)=2C\sqrt{2E-q_2^2+\tfrac{2}{3}q_2^3} . \end{aligned} \tag{11}$$

If we consider the crossing point distribution on $q_2=0$, $D(q_1,p_1)$, a similar discussion leads to the cross section distribution $d(q_1)$:

$$d(q_1)=2C\sqrt{2E-q_1^2} . \tag{12}$$

If we are only concerned with the cross section distribution between $q_i=a$ and b, we may use the normalized distribution

$$\rho(q_i)=\frac{d(q_i)}{\int_a^b d(q_i)dq_i} \tag{13}$$

to discuss the ergodicity of this region. Note that this ρ has a different meaning from that in (5). In the following section, we shall focus on the numerical discussion of statistical properties (ergodicity) in our modified Henon-Heiles model in the q_1-p_1 and q_2-p_2 planes.

III. NUMERICAL RESULTS: DEGREE OF ERGODICITY

For the case $E \leq \frac{1}{6}$, the motion is bounded inside an equilateral triangle domain surrounded by three lines: $q_2=\sqrt{3}q_1+1$, $q_2=-\sqrt{3}q_1+1$, $q_2=-\frac{1}{2}$. When E exceeds $\frac{1}{6}$, the oscillator will escape from the saddles. Thus we choose the boundary of the form

$$(q_2+\sqrt{3}q_1-\lambda)(q_2-\sqrt{3}q_1-\lambda)(q_2+\lambda/2)=0\ . \tag{14}$$

$\lambda=1$ corresponds to the case of the natural boundary (at $E=\frac{1}{6}$). We also discuss the cases $\lambda>1$, when the particle will escape from the saddle points $(q_1,q_2)=(0,1)$, $(\pm\sqrt{3}/2,-1/2)$ and be reflected elastically by the boundary. For cases $\lambda \gg 1$, the motion approaches the Henon-Heiles motion without reflecting walls in the large E region (the walls play a role only in restricting the trajectory in a finite domain; they do not essentially affect the dynamics in the region of small $|q_1|$ and $|q_2|$). Figure 1 gives two kinds of walls corresponding to $\lambda=1$, $\lambda=2$, respectively. In our computation, we integrate the equations of motion by the Runge-Kutta method, and the time step is adjusted according to different energies to keep the accuracy of the integration.

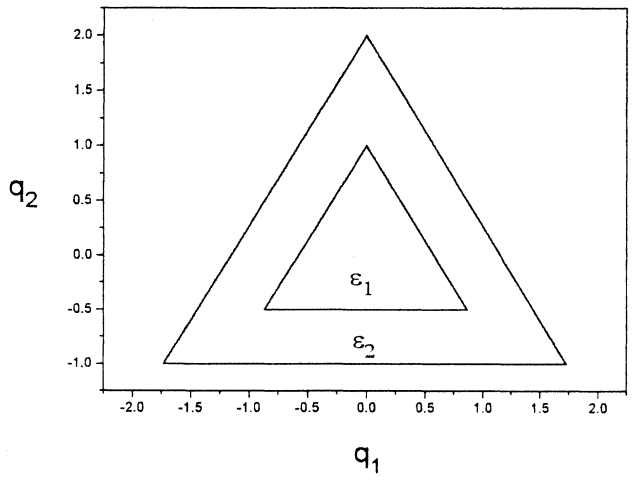

FIG. 1. Two kinds of reflecting walls used to discuss the ergodicity of Henon-Heiles systems. Boundary ϵ_1 corresponds to $\lambda=1$ and ϵ_2 to $\lambda=2$. (0,1), $(\pm\sqrt{3}/2, -\frac{1}{2})$ are three saddle points of the original Henon-Heiles model at $E=\frac{1}{6}$.

A. Investigation of ergodicity by changing energy with walls fixed

Figures 1(a) and 2(b) give the Poincaré sections ($q_1=0$, $p_1>0$) for energies $E=\frac{1}{5}$ and $\frac{1}{2}$ in the natural boundary case (ϵ_1). A comparison of Figs. 2 with similar figures of cross sections presented in earlier papers (e.g., see Figs. 8.5, 8.6, and 8.7 of Ref. [1]) is interesting. When E increases from $E=\frac{1}{6}$, the motion approaches a more chaotic one at first, and then for sufficiently large energy new KAM tori appear and the motion becomes less chaotic. In fact, for very large energy, the region covered by a chaotic trajectory on the energy surface becomes very small, and the system approaches an integrable one. This behavior seems quite different from those usually expected (with increasing energy, KAM tori would usually be destroyed and eventually the system would reach ergodi-

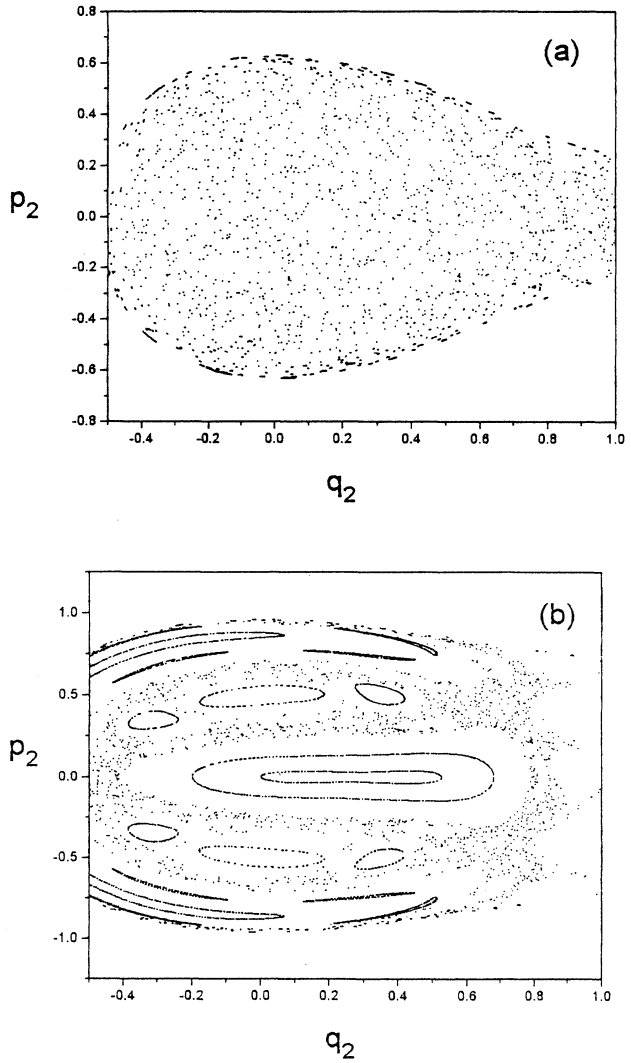

FIG. 2. Poincaré cross section ($q_1=0$, $p_1 \geq 0$) for the ϵ_1 boundary case with (a) $E=\frac{1}{5}$ and (b) $E=\frac{1}{2}$.

city). But considering the effect of the reflecting wall, we may easily explain this result. This is mainly due to the competition of the kinetic energy of the particle and the nonlinear anharmonic potential. When E becomes very large, the kinetic energy term becomes dominant, and the portion of the harmonic potential energy and nonlinear interaction becomes negligible. When $E \to \infty$, the Henon-Heiles system just corresponds to an equilateral triangle billiard, i.e., a free particle moving inside the equilateral triangle boundary. This billiard system is integrable, which has been verified both theoretically and numerically [2].

In Figs. 3(a)–3(d), we compare the numerical and microcanonical distributions $\rho(q_2)$ for different energy cases. Here each numerical $\rho(q_2)$ is obtained by running a single trajectory, 5×10^5 points on the cross section are collected for the statistics, and q_2 ranges from $-\frac{1}{2}$ to 1. At $E=\frac{1}{5}$, we find that the two curves are in good agreement with each other, which indicates that the system is almost completely ergodic. When $E=\frac{1}{2}$, large deviation occurs, which means that ergodicity is destroyed again for high-energy cases.

Figure 4 gives the differences between the numerical cross section distribution and the theoretical canonical distribution for the case of the boundary $\epsilon_1(\lambda=1)$, $\epsilon_2(\lambda=2)$. The difference is defined as

$$\Delta=\int_a^b |\rho_{\text{num}}(q_i)-\rho_{\text{mic}}(q_i)|dq_i \ . \tag{15}$$

In the ϵ_1 case, we find that for small and large energies Δ is large, whereas for $E\in(\frac{1}{6},\frac{1}{4})$ Δ becomes very small, and a minimum exists at $E=0.225$, i.e., the system approaches the highest degree of ergodicity. For $E>\frac{1}{4}$, Δ increases with increasing E, and the system approaches

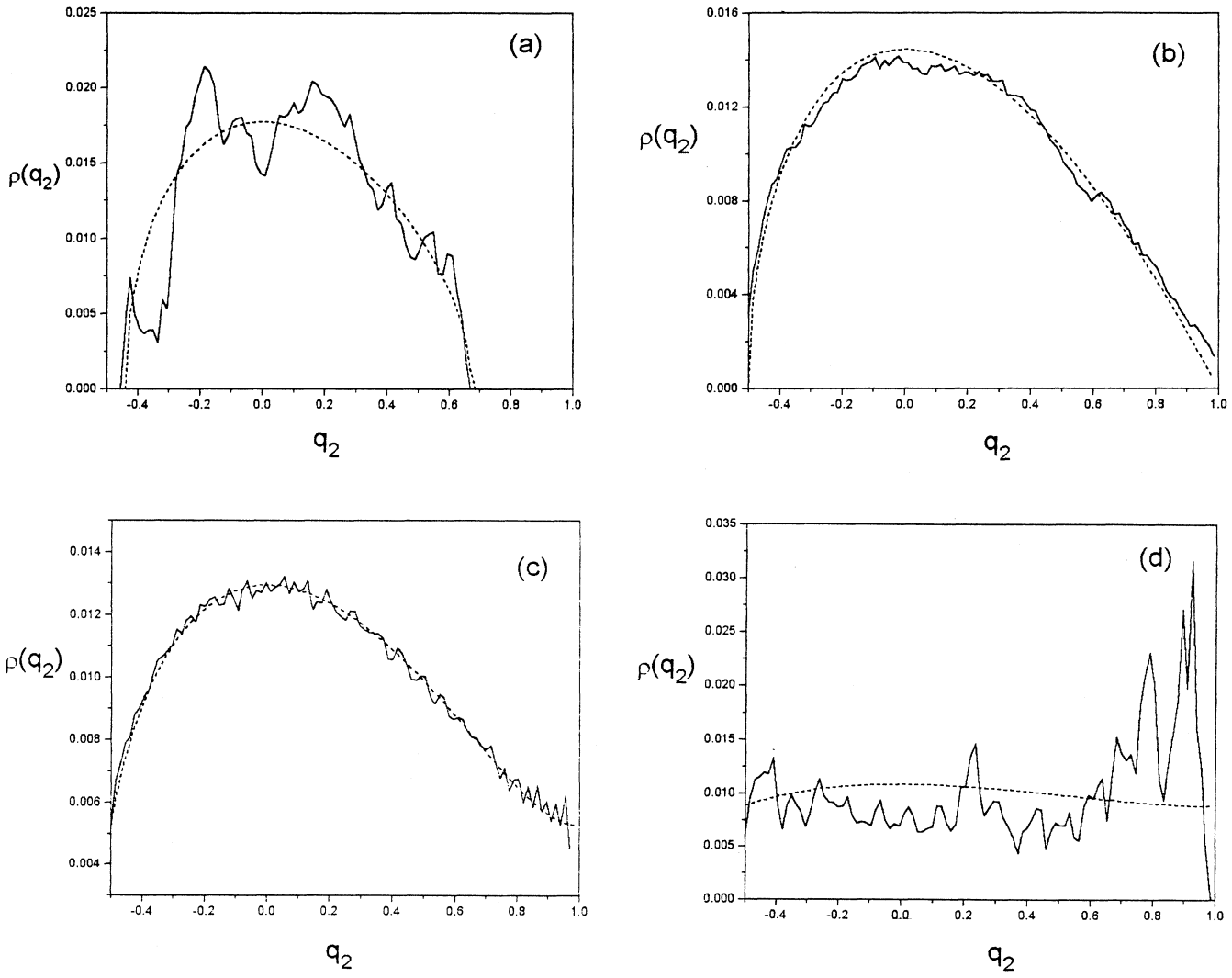

FIG. 3. A comparison of theoretical (dashed curves) and numerical distribution $\rho(q_2)$ (solid curves) for different energies $E=\frac{1}{8}$ (a), $E=\frac{1}{6}$ (b), $E=\frac{1}{5}$ (c), and $E=\frac{1}{2}$ (d). Good agreement is shown in (c). For lower and higher energies, deviations are large, indicating nonergodicity.

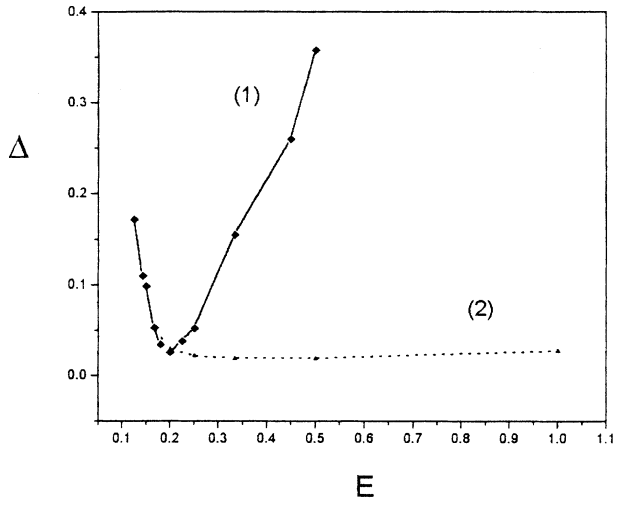

FIG. 4. The difference Δ versus energy E for walls (1) ϵ_1 ($\lambda=1$) and (2) ϵ_2 ($\lambda=2$). A narrow valley for the ϵ_1 boundary and a wider one for the ϵ_2 boundary can be seen.

an integrable one. This tendency is due to the boundary effect. When we use the boundary ϵ_2 (see curve 2 in Fig. 4), we find that the valley of the V-shaped line shifts towards larger energy, and the valley becomes wider and deeper. This means a better ergodicity can be achieved for larger boundary cases; this fact will be shown in more detail in the following subsection.

B. Investigation of ergodicity by changing walls with energy fixed

It has been shown that ergodicity can be achieved in a large energy range if λ increases. With increasing λ, the effect of reflecting walls decreases, and the bounded motion approaches the behavior of the unbounded Henon-Heiles model in the small $|q_1|, |q_2|$ region. In Figs. 5(a)–5(c), the Poincaré cross sections ($q_2=0$, $p_2>0$) are shown at $E=\frac{1}{2}$ for different λ. We find that the system tends to be more ergodic on the energy surface with increasing λ. This ergodic property can be seen more easily in Figs. 6(a)–6(c). $\rho(q_1)$ is a semielliptic distribution for $\lambda \geq \sqrt{6E}$ if the system reaches ergodicity.

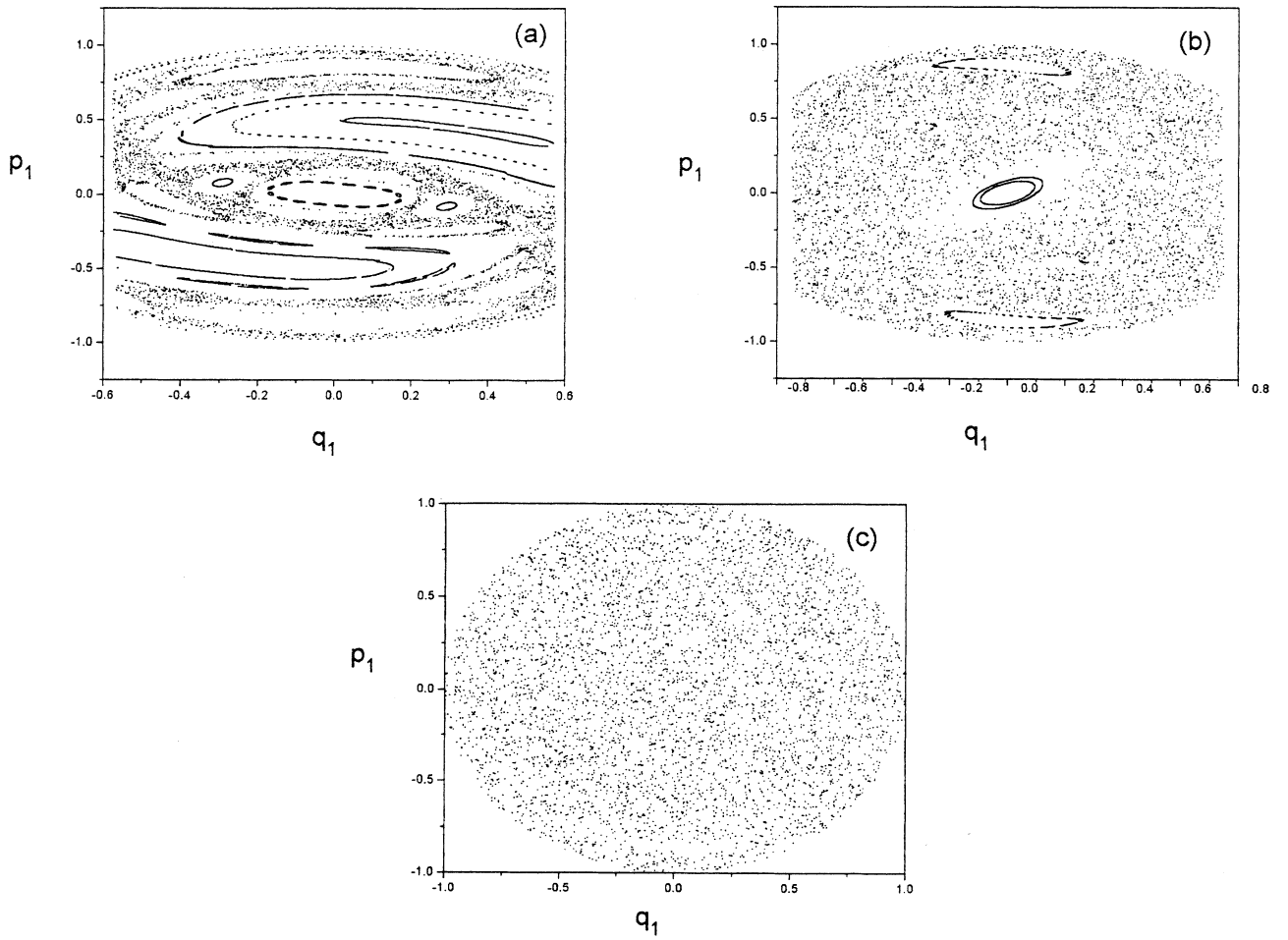

FIG. 5. Poincaré cross section ($q_2=0$, $p_2 \geq 0$) at $E=\frac{1}{2}$ for equilateral triangle reflecting walls with different dimensions. (a) $\lambda=1.0$, (b) $\lambda=1.3$, and (c) $\lambda=1.732$. With increasing λ, the Henon-Heiles system quickly reaches ergodicity.

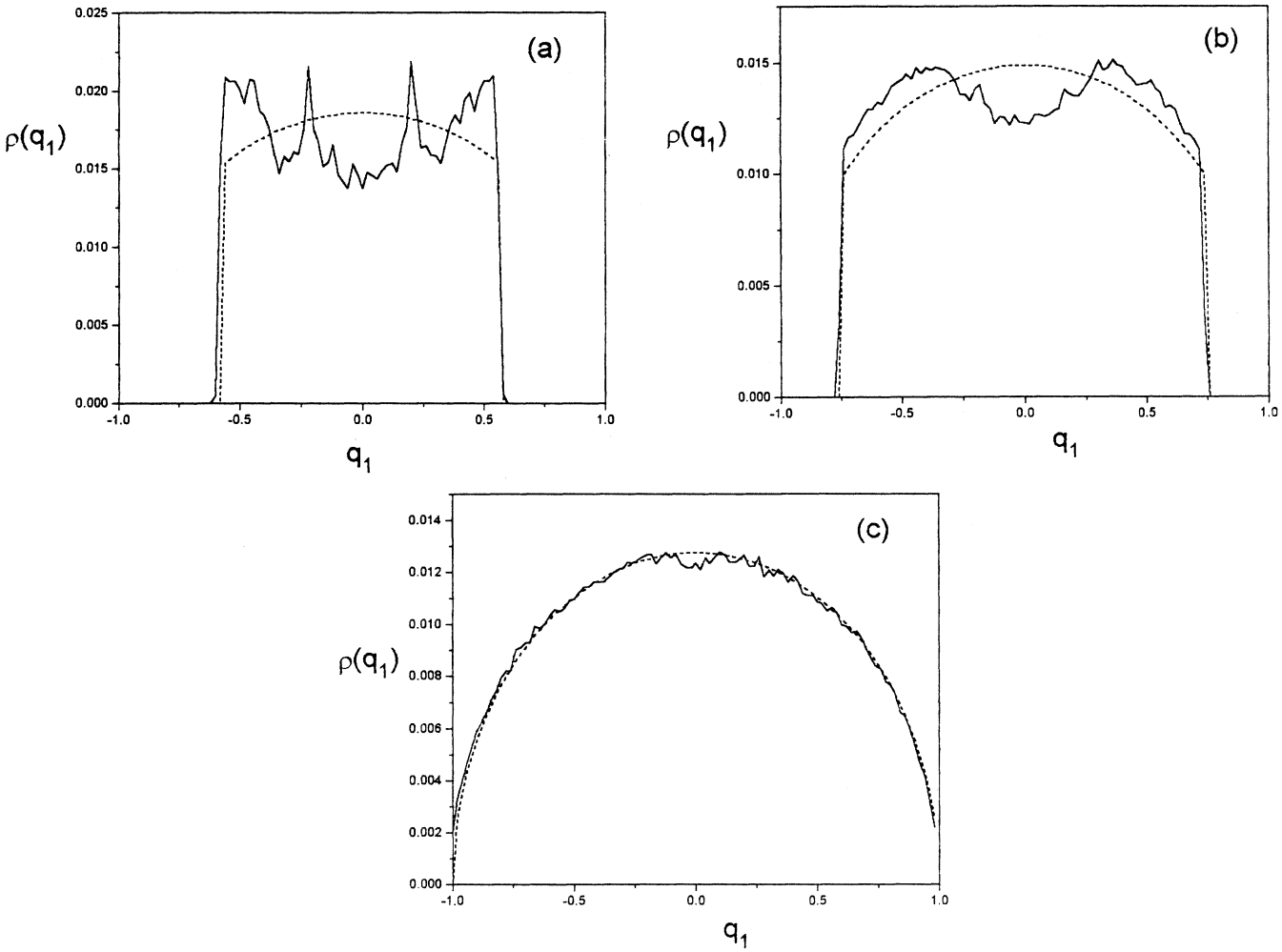

FIG. 6. A comparison of theoretical and numerical distribution $\rho(q_1)$ at $E=\frac{1}{2}$ for different λ. The choice of λ is the same as in Fig. 5. Good agreement is shown for larger λ.

As λ increases, the degree of erogodicity increases. This tendency is more clearly shown in Fig. 7, where the differences Δ versus λ are shown for $E=\frac{1}{2}$ and $\frac{2}{3}$. We find that Δ decreases sharply within a rather narrow λ range, and this sharp drop turns to be parallel to the λ axis when λ continues to increase. It seems to us that on this minimum Δ a perfect ergodicity is achieved. Increasing E and λ can no longer reduce Δ, but Δ can be further reduced by increasing the number of crossing points (e.g., when we use 10^6 crossing points for statistics, we can get $\Delta_{\min}\approx 0.0198$, smaller than that in Fig. 7); this suggests that this minimum Δ might be due to statistical error.

IV. CONCLUSIONS

In this paper, we suggest a class of nonlinear coupling oscillator models with reflecting walls, and thus ergodic properties at various energies E can be fully investigated. We find that the modified Henon-Heiles system possesses quite good ergodic properties at large energy in the phase space regions far from the reflecting boundary. On the

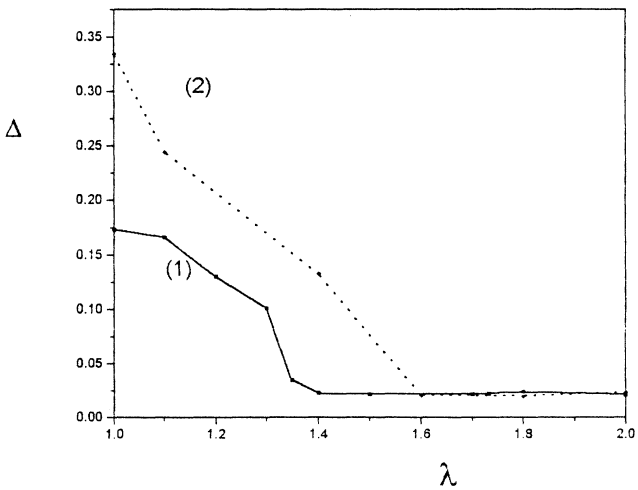

FIG. 7. The difference Δ versus λ for energies (1) $E=\frac{1}{2}$ and (2) $E=\frac{2}{3}$. Δ drops quickly with increasing λ, indicating that the system reaches ergodicity in a small range of λ. The two curves reach the same asymptotic Δ value in the large λ region.

other hand, we suggest a quantitative method for estimating the degree of ergodicity. This method is efficient and has good physical meaning. By comparing the microcanonical ensemble distribution and numerical statistical distribution, the ergodicity of a dynamic system may be explicitly and quantitatively described. This method is especially useful for dynamic systems with large degrees of freedom. It should be mentioned that the shape of the reflecting wall will strongly influence the chaotic and ergodic behavior of the dynamic system. Influenced by both the nonlinear coupling and the shape of the boundary, the motion of the system will become complicated as well as interesting and significant. These phenomena will be discussed in the future.

[1] L. E. Reichl, *A Modern Course in Statistical Physics* (University of Texas Press, Austin, 1980).
[2] L. E. Reichl, *The Transition to Chaos: In Conservative Classical System: Quantum Manifestations* (Springer-Verlag, Berlin, 1992).
[3] M. C. Gutzwiller, *Chaos in Classical and Quantum Mechanics* (Springer-Verlag, Berlin, 1990).
[4] R. Z. Sagdeev, D. A. Usikov, and G. M. Zaslavsky, *Nonlinear Physics: From the Pendulum to Turbulence and Chaos* (Harwood Academic, Chur, Switzerland, 1988).
[5] V. L. Berdichevsky, J. Appl. Math. Mech. **52**, 738 (1988).
[6] Ya. G. Sinai, Dokl. Akad. Nauk SSSR **153**, 1261 (1963) [Sov. Math. Dokl. **4**, 1818 (1963)].
[7] Ya. G. Sinai, Usp. Mat. Nauk **25**, 141 (1970) [Russ. Math. Surv. **25**, 137 (1970)].
[8] D. Szasz, Physica A **194**, 86 (1993).
[9] L. Bunimovich, C. Liverani, A. Pellegrinetti, and Y. Suhov, Commun. Math. Phys. **146**, 357 (1992).
[10] N. Simanyi and D. Szasz, J. Stat. Phys. **76**, 587 (1994).
[11] J. L. Vega, T. Uzer, and J. Ford, Phys. Rev. E **48**, 3414 (1993).
[12] T. Kawabe and S. Ohta, Phys. Rev. A **41**, 720 (1990).
[13] B. Henry and J. Grindlay, Phys. Rev. E **49**, 2549 (1994).
[14] M. Henon and C. Heiles, Astron. J. **69**, 73 (1964).
[15] V. L. Berdchevsky and M. V. Alberti, Phys. Rev. A **44**, 858 (1991).
[16] M. Pettini and M. Landolfi, Phys. Rev. A **41**, 768 (1990).